doi:10.20944/preprints202104.0617.v1

Article

Parameter Estimation of a Single-Phase Boost PFC Converter with EMI Filter based on an Optimization Algorithm

Gabriel Rojas-Dueñas [1], Jordi-Roger Riba [1] and Manuel Moreno-Eguilaz [2,*]

[1] Universitat Politècnica de Catalunya, Electrical Engineering Department, Rambla Sant Nebridi 22, 08222 Terrassa; gabriel.esteban.rojas@upc.edu; jordi.riba-ruiz@upc.edu
[2] Universitat Politècnica de Catalunya, Electronics Engineering Department, Rambla Sant Nebridi 22, 08222 Terrassa; manuel.moreno.eguilaz@upc.edu
* Correspondence: manuel.moreno.eguilaz@upc.edu; Tel.: +34-937-398-365

Abstract: This paper proposes an approach to estimate the parameters of an AC-DC boost power factor corrector converter which includes an EMI filter. To this end, once the topology is known, measurements at the input and output terminals of the converter are done to identify the values of the passive elements. The proposed methodology is based on the trust-region nonlinear least squares algorithm to identify the parameters of the converter. The steady-state and the transient signals of the converter at the input/output terminals are acquired non-intrusively without any internal modification of the circuitry. The accuracy of the parameter identification carried out is determined by comparing the estimated values with the actual values provided by the manufacturer, and by contrasting the measured signals with the ones obtained with a simulation model with the estimated values of the parameters. The results presented in this paper prove the accuracy of the proposed approach, which can be extended to other power converters and filters.

Keywords: power factor correction; EMI filter; parameter identification; boost converter

1. Introduction

Power factor corrector (PFC) converters are devices aimed to improve the power quality of a distribution system by increasing the power factor and decreasing the total harmonic distortion (THD) [1,2]. They are mainly used in applications feeding a large number of electronic loads for different applications including low power industrial sectors, residential and commercial distribution systems. These electronic loads generate harmonic currents and inject reactive power to the electrical system, thus resulting in a low power factor and high THD [3]. In these scenarios, the inclusion of a PFC converter is necessary in order to comply with the international power quality standards, such as the IEEE Std. 519 [4]. In particular, boost PFCs are widely used in household appliances, laptop adapters, on-board chargers and aircraft power supply, among others [5]. When supplying switching-mode power converters such as the boost PFC, it is required to add an electromagnetic interference (EMI) filter at its input in order to attenuate the conducted EMI disturbances generated by the electronic equipment towards the power line [6] and fulfill the stringent requirements of EMI-related international standards. Companies of the aforementioned sectors, typically integrate the boost PFC and EMI filters to systems that include many other power devices and components from different manufacturers. These companies need accurate models of their devices to perform several tasks, such as the design of controllers, predictive maintenance, calculation of the energy consumption, etc. [7]. However, manufacturers of power devices often do not provide enough information regarding the topology or the inner components characteristics due to confidentiality reasons [8]. To generate accurate discrete models of power electronics devices used during the design and optimization stages, engineers require to know the values or parameters of the constitutive components in advance [9]. Therefore, it is highly appealing to develop a method to estimate these values in order to develop models to replicate the behavior of power electronics devices with high accuracy.

At the most authors knowledge, there are no studies dealing with the topic of parameter identification of a boost PFC with an input EMI filter. However, the literature includes different approaches aimed to identify the parameters of switched mode power converters, such as buck, boost or buck-boost converters. In [10] and [11] the authors proposed an estimation method based on obtaining state space averaging models of the converters, where the topology of the converter is used to obtain a transfer function that is tuned using the measured data. In [7], the parameters of a buck and a boost converter are identified by calculating the analytical equations of the circuits, although this an intrusive approach since it measures the current flowing through the inductor of the converter. Ahmeid et. al. [12] performed a real time estimation of a transfer function that represents a synchronous buck converter by using a Kalman filter. In [13] the authors use a dichotomous coordinate descent method to perform an online identification of the voltage transfer function, although an external excitation of the DC-DC converter is required. In [14], the passive and parasitic elements of DC-DC converters are calculated by means of a continuous time model that applies a polynomial interpolation. In [15] a buck converter is modeled by means of a NARX neural network. However, the parameters are not identified since it obtains a black-box model. In [16], a parameter estimation of a buck, a boost and a buck-boost converter is carried out by applying an optimization algorithm that identifies the values of the passive elements. Authors in [17] present a review of the state-of-the-art of parameter identification methods for DC-DC power converters, although despite the accurate results, all the mentioned approaches are invasive or intrusive since they require external excitations or internal measurements of the converter.

On the other hand, the technical literature reveals that most of the works conducted on EMI filters, either identify the filter from a simplified transfer function [18] or perform an electromagnetic analysis of the filter components [19,20], thus do not being practical to obtain the actual values of the filter parameters. It is straightforward to deduce that there is an imperious need to non-intrusively identifying at once all parameters of the electronic device from the input/output voltages/currents, because the input/output terminals are often the only accessible points.

This paper proposes identifying all the parameters of a boost PFC converter with an EMI filter stage. It is based on an optimization algorithm that uses non-intrusive measurements from the converter and the filter, since it only acquires the data from the input and output terminals. A methodology that comprises four different optimization stages is also proposed, which uses the trust-region non-linear least squares algorithm. The paper demonstrates that it is possible to simulate the behavior of the PFC converter with high fidelity once the set of parameters has been identified.

This work contributes to the state-of-the-art in several aspects. First, it proposes a strategy to estimate more than 30 parameters based on non-intrusive measurements at the input and output terminals of the different elements of the PFC converter. Second, the different elements of the control loops (voltage and current) are identified, which allows to reproduce with high accuracy the transient behavior of the converter. Third, estimating all the parameters of a widely used device, such as a AC-DC PFC, results advantageous in the design and maintenance of systems supplying multiple electronics loads. Fourth, the algorithm is also capable of identifying the values of the parasitic components of the converter, which is useful for high-frequency switching devices as the one studied in this paper. Finally, the experimental setup to perform the data acquisition is relatively simple because it is not necessary to apply internal excitations to the circuit or perform invasive measurements in the inductor of the boost converter

2. The AC-DC Power Factor Correction Converter

 doi:10.20944/preprints202104.0617.v1

The boost PFC analyzed in this paper is an AC-DC converter used to obtain an output DC voltage from an AC source with a high power factor [21]. This converter is widely used because it is capable of supplying power to multiple loads while regulating continuously the output voltage [22], being desirable in many industry applications. The boost PFC is a switched mode power converter (SMPC) that uses pulse width modulation (PWM) to convert efficiently the electrical power. A side effect of this conversion is the generated high-frequency switching harmonics, which induce the parasitic characteristics of the different elements in the circuit. Also, it introduces electromagnetic interference (EMI) to the converter, which is a disturbance affecting electric and electronic circuit by conduction, electromagnetic induction or electrostatic coupling, which tends to degrade the behavior of such circuit. Then, to mitigate this interference and to satisfy the EMI standard, it is necessary to add an EMI filtering stage at the input of the boost PFC converter.

Figure 1 shows the block diagram of the power converter to be identified in this paper. It is divided in four different stages, each one including different physical and non-physical parameters to be identified. These four stages are the EMI filter, the single-phase AC-DC rectifier, the DC-DC boost converter and the control loop of the SMPC converter.

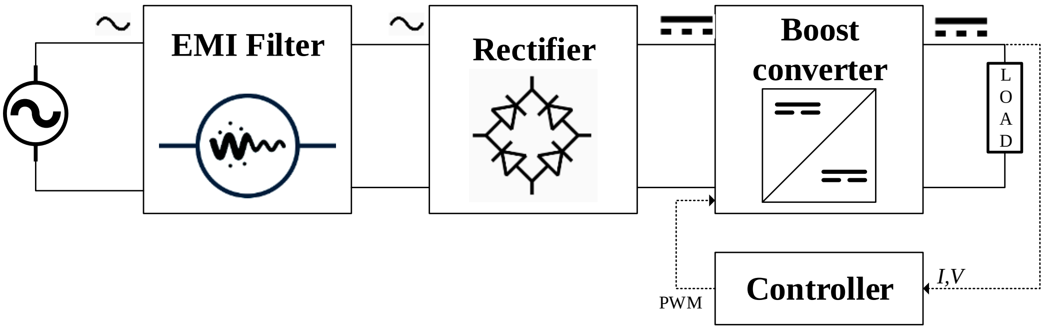

Figure 1. Block diagram of the boost PFC which includes an EMI filter

The topologies of the EMI filter and the boost PFC converter are based on commercially available components. The first one is the power line filter model 10VN1, manufactured by Corcom. It consists of an EMI filter that is used between the power line and the electronic equipment to attenuate the conducted EMI disturbances generated by the electronic equipment towards the power line [6]. In this paper, an EMI/RFI power line filter is analyzed, which is designed for providing differential- and common-mode attenuation for digital equipment such as switching power supplies, over the 10 kHz – 30 MHz frequency range. Figure 2 shows the circuit of the EMI filter used as the input stage of the boost PFC. It is seen that there are 12 unknown parameters to be identified corresponding to the passive elements of the circuit. Normally, the values of the coupled inductors (i.e. L1 and L2) and the capacitors with common ground (i.e., C3 and C4) are identical, thus reducing the number of parameters to be estimated and simplifying the identification process.

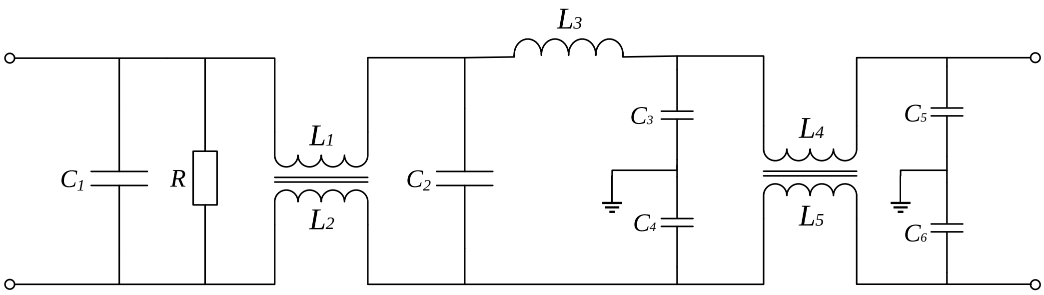

Figure 2. EMI filter to be identified

Preprints (www.preprints.org) | NOT PEER-REVIEWED | Posted: 22 April 2021 doi:10.20944/preprints202104.0617.v1

The AC-DC boost PFC converter consists of a single-phase rectifier connected to a step-up high-frequency switching DC-DC converter that is regulated by means of two control loops (voltage and current). The boost PFC converter studied in this paper is the evaluation module model ISA102V2 manufactured by ST, which is an 80 W high performance transition mode PFC board based on the L6562A controller. The AC-DC conversion is done by means of a full wave diode bridge with an output capacitor for smoothening the rectified voltage. The rectifier feeds a boost converter with a classic topology that includes the parasitic resistance of the capacitor and the inductor. Due to the high-switching frequencies of the transistors, it is also important to consider the parasitic resistance of these elements.

Figure 3 presents the circuit of the boost PFC and the elements to be estimated. Regarding the rectifier, the exponential model of the diode was used since it represents accurately its behavior [23]. It relates the current that flows across the diode to its voltage drop as,

$$I = I_s \cdot \left(e^{qV/(NkT_m)} - 1 \right) \tag{1}$$

where I and I_s refer to the diode current and saturation current, respectively, V is the voltage drop across the terminals of the diode, q is the elementary charge of an electron, k is the Boltzmann constant and T_m is the working temperature.

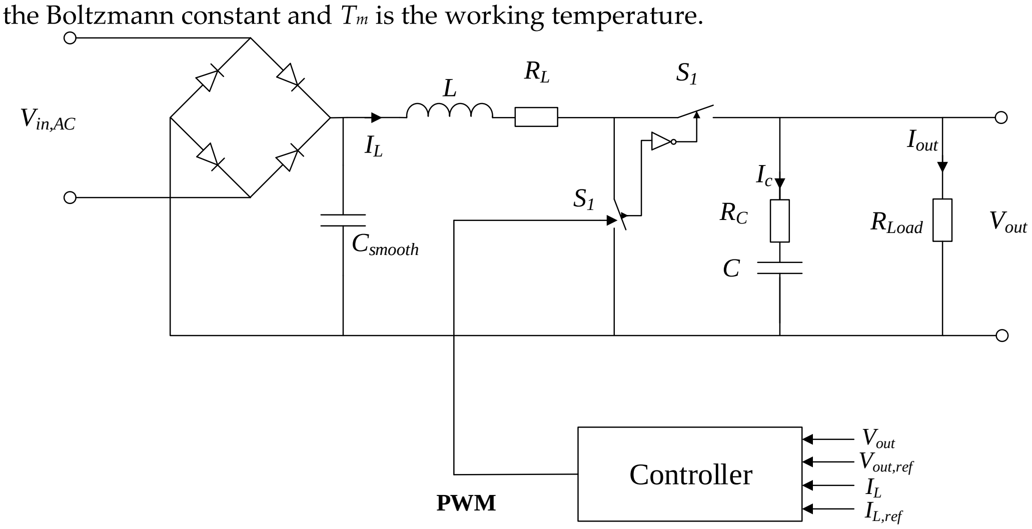

Figure 3. Boost PFC to be identified

The controller of the DC-DC converter has two main objectives. The first one is to maintain a power factor close to 1 by using an inner current control loop, so the input voltages and currents should be almost in phase. The second objective is to deliver a constant output voltage by means of an outer voltage control loop [24]. It regulates the output voltage to a given reference value. Both loops apply a PI compensation, thus, creating a robust control scheme of the boost PFC converter.

Figure 4 presents the block diagram of the controller along with its circuitry implementation. Regarding the parameters to be estimated, the current control is a PI compensation because it is normally implemented in the microcontroller unit of the converter and it can be modeled as a transfer function. Figure 4 indicates that the reference value of the inductor current is given by the output generated by the outer voltage loop, showing how both control loops are interconnected. The compensation of the outer voltage control loop is performed by a type 3 operational amplifier, as shown in Figure 4. (b). This type of compensation provides two poles and two zeros, being used when a phase boost greater than 90 degrees is needed [25]. The reference voltage is specified by design and the values of the resistors and capacitors must be identified.

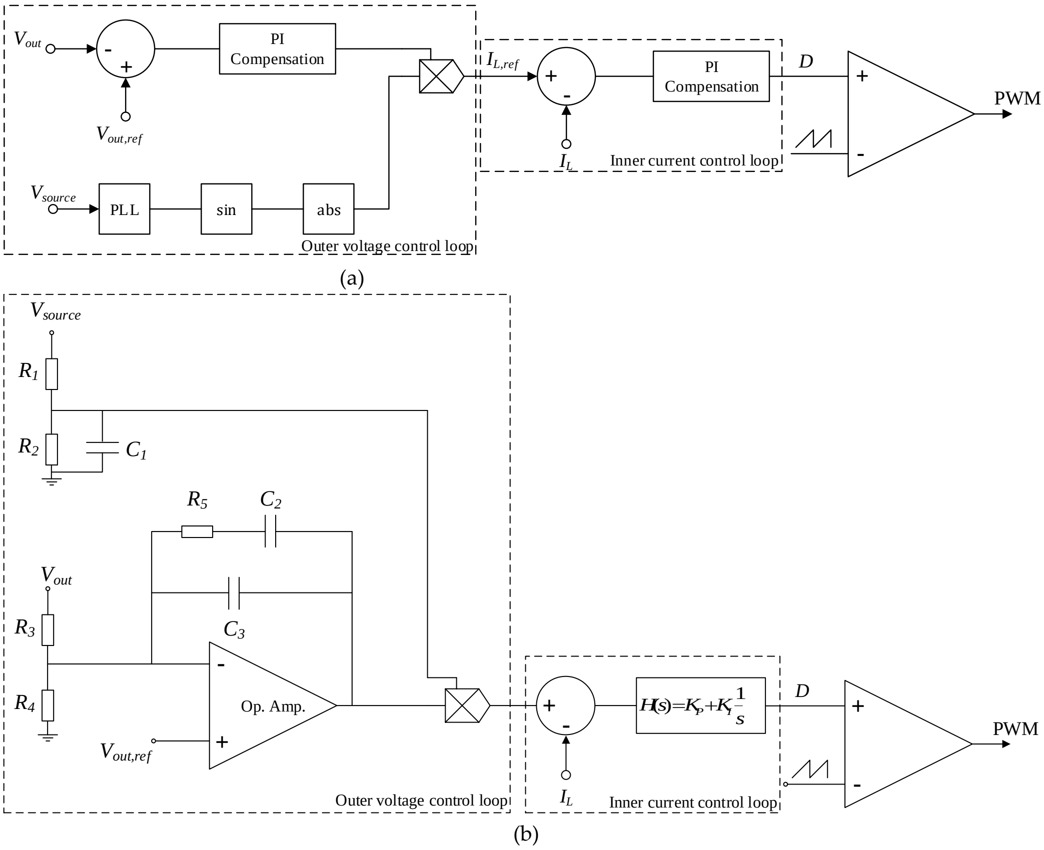

Figure 4. Boost PFC controller. (a) Block scheme. (b) Circuit

Given the topologies of the four blocks presented in this section, there are 33 unknown values to be estimated. They correspond to the parameters of the EMI filter $(R, C_1, C_2, C_3, C_4, C_5, C_6, L_1, L_2, L_3, L_4, L_5)$, the single phase rectifier $(I_S, N, T_m, R_{diode}, C_{smooth})$, the boost converter $(C, R_C, L, R_L, R_{S1}, R_{S2})$ and the control loops $(R_1, R_2, R_3, R_4, R_5, C_1, C_2, C_3, K_P, K_I)$. The following Sections present the proposed methodology to identify these sets of parameters and the data acquisition procedure.

3. The Proposed Parameter Estimation Methodology

This section presents the proposed approach to identify the parameters of the boost PFC converter. First, it introduces and explains the main core of the parameter identification strategy, which is the nonlinear least squares (NLS) optimization algorithm. The second part of this section describes the proposed methodology.

3.1. Nonlinear least squares optimization for parameter estimation

This section presents the algorithm that is used in this paper to estimate the parameters of the boost PFC converter. It is well-known that switched mode power converters, as the one analyzed in this paper, have nonlinear characteristics, preventing conventional parameter estimation methods of obtaining accurate results [26]. Thus, the trust-region-reflective least squares algorithm is used because it is able to deal with nonlinearities. It is mainly used to tune parameters of constrained nonlinear problems. The algorithm finds a set of variables x with the purpose of minimizing an objective function [27] given by:

$$\min_x E(x) = \min_x \left(\sum_{i=1}^{n} e_i^2(x) \right) \quad (2)$$

where $e_i(x)$ refers to the error function, which is defined according to the type of problem. It is constrained by the lower and upper bounds of the variables, in the form of $lb \leq$

$x \le ub$ [16]. The optimization approach aims to replicate the behavior of $e(x)$ in a neighborhood *N* (trust-region) by means of a quadratic function $q(s)$ [28]. The main purpose of this algorithm is to expand the Taylor series of *q(s)* and to obtain the trust-region of the problem. The region *N* is generated around the actual value of x_k and consequently, the main challenge of the iterative process is to find the x_{k+1} point within the *N* neighborhood. The selection of the new point must satisfy $e(x_{k+1}) < e(x_k)$, otherwise, the trust-region *N* is reduced and the point x_k does not change. Therefore, a proper selection of the iteration step $s_k = x_{k+1} - x_k$ is needed, which is obtained by solving the subproblem,

$$\min_{s \in N} q_k(s) = \min_{s \in N}\left(g(x)^T s + \frac{1}{2}s^T H(x)s\right) \tag{3}$$

where *g(x)* and *H(x)* correspond to the gradient and the Hessian matrix of *e(x)* evaluated in x_k, respectively. The condition $s \in N$ can be expressed in the form of $\|D_k^{-1}s\| < \Delta_i$, *D* being the diagonal scaling matrix, and Δ_i the size of the trust-region. *D* is calculated by means of the vector function, which is defined by $v(x) = [v_1(x), v_2(x), \dots, v_n(x)]^T$ and it is obtained depending on the gradient of the error function, the boundaries (*ub* and *lb*) and the actual state x_k [16]. Thus, for a given x_k, the value of s_k is calculated by using (3) and $x_{k+1} = x_k + \alpha_k s_k$, where α_k represents the step length. This length merely depends on the interior of *N* (int(*N*)), which is defined by the upper and lower bounds of the variables being optimized. The iterative process carried out to find the minimum value of *e*(*x*) is the reflective line search (RLS), which determines how the iterations move over the boundary of int(*N*). To accelerate the convergence of the optimization, the space int(*N*) is limited to a subspace *V* of two dimensions. This restriction enhances the speed of the algorithm because the mathematical calculations of the eigenvectors and eigenvalues are easier due to the low dimension of the subspace [29]. Also, by using a 2-D subspace, the problem can be solved with well-known and less complex algorithms such as the preconditioned conjugate gradient method. Furthermore, the Jacobian matrix *J*(*x*) approximates the Hessian matrix *H*(*x*) and it is calculated by means of the efficient finite differencing method [28]. The initial or seed point defined prior to the optimization process plays an important role in the trust-region reflective algorithm since it determines the step length and how the trust-region reduces after each iteration. Therefore, the local minimum reached after the NLS optimization is conditioned by the initial value of the variables x_0.

Considering the characteristics of the boost PFC converter mentioned in the previous subsection, and the data that can be retrieved from it, the objective function of the parameter identification problem is defined as follows:

$$\min_x\left(\sum_{i=1}^{n}\left(\left(V_{in}^{est}(t)+I_{in}^{est}(t)+V_{out}^{est}(t)+I_{out}^{est}(t)\right)-\left(V_{in}^{meas}(t)+I_{in}^{meas}(t)+V_{out}^{meas}(t)+I_{out}^{meas}(t)\right)\right)^2\right), t = iT \tag{4}$$

Here *V* refers to the voltage and *I* to the current, the subscripts denote the port where the signals are obtained and the superscripts indicate whether the signal is estimated by the model or acquired in the laboratory, *n* represents the total number of time-steps considered, *T* is the length of the time step and *t* is the time instant where the error function is being evaluated. The variables *x* to be optimized are the values of the electrical elements of the EMI filter and boost PFC converter, and the control parameters mentioned in subsection 2.1. The minimum and maximum values of these variables define the trust-region *N* of the NLS optimization. However, if all the variables are identified at once, *N* would be too large and the problem too complex to solve, then, next subsection presents the proposed methodology to identify all the parameters.

3.2. Proposed parameter identification methodology

Given the complexity of the circuit and the extensive number of variables to be identified, it is necessary to define a methodology that allows the identification of all the parameters with high accuracy and without comprising the total simulation time. Identifying all parameters at once may lead to an incorrect solution because it is very likely that the optimization approach finds a local minimum that differs from the actual parameters of the converter.

Figure 5 shows the proposed algorithm, which aims to identify certain sets of parameters separately in order to reduce uncertainty and obtain better results.

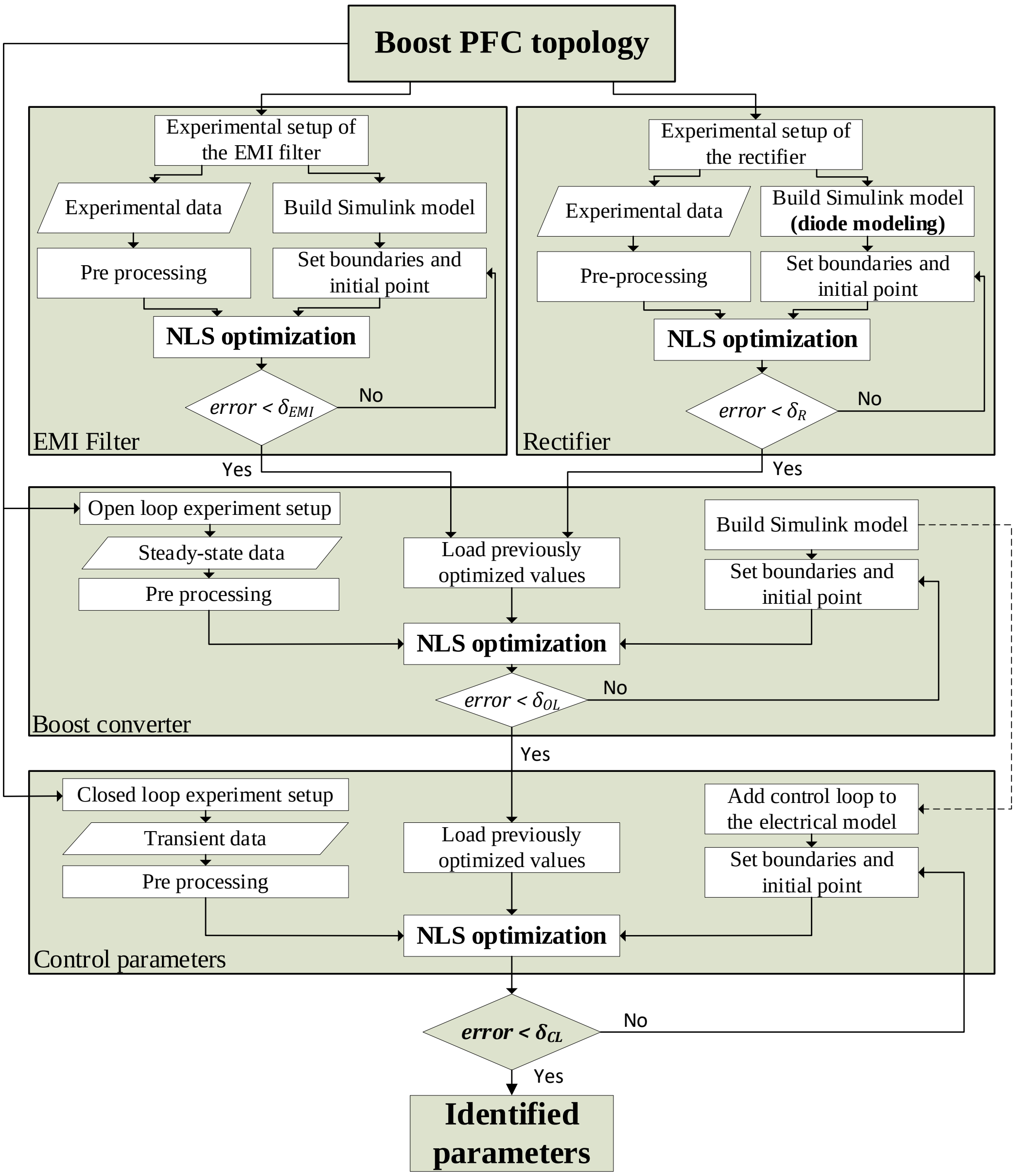

Figure 5. Proposed methodology to identify the parameters of the boost PFC converter.

The algorithm is divided in four different parts, which correspond to the four blocks of the diagram shown in Figure 1 (EMI filter, rectifier, boost converter and the controller). The first step of the methodology is to define the circuit topology of all components and to specify the variables to be estimated. This was done in Subsection 2.1, where a detailed description of each component is shown, as well as the unknown parameters. The next step is to identify the parameter values of the EMI filter and the rectifier, these being independent processes, which can run in parallel. The third stage corresponds to the open loop parameter estimation of the boost converter, where the previously identified values and topologies of the EMI filter and rectifier are used. Finally, the control or closed loop parameters of the converter are estimated using the NLS algorithm and the previously obtained parameters. A thoroughly explanation of each optimization stage is given as follows:

- EMI filter: This stage aims to identify the 12 values of the passive elements of the EMI filter. Firstly, the experimental setup and the data to be acquired in the laboratory are defined. To force a sufficient rich response of the EMI filter that enables identifying its parameters, a capacitor was connected at the output terminals in parallel with the resistive load when a periodic square waveform voltage was applied to the input terminals by means of an AC source. To perform the identification process, the voltage and current at the input and output terminals are needed. To simulate the high output impedance of the function generator used to generate the square waveform, a resistance R_{in} in series with an inductance L_{in} was added to the Simulink® model, and the values of such parameters were identified jointly with the parameters of the filter. To enhance the performance of the identification process, the data is divided into two sets, which are used in the optimization process, i.e., the data centered in the rising edge of the periodic square waveform, and in the falling edge of the period. This is done to avoid using a complete period of the signals by focusing on the intervals that contain the relevant information. Figure 6 shows the Simulink® model used to identify the parameters of the passive EMI filter.

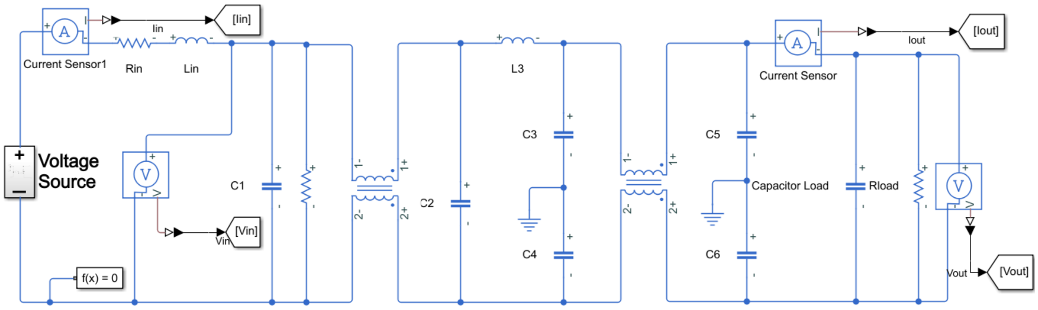

Figure 6. Simulink model of the EMI filter

- Rectifier: The identification process of the parameters of the single-phase rectifier is independent from the other elements of the boost PFC converter, since it just uses the acquired signals at the input and output terminals of the rectifier. This process aims to estimate the diode and the output capacitor parameters. The complexity of this stage depends on the diode model that is considered, which in this case is the exponential, as described by (1).
  The parameter estimation uses the data of three different experiments of the rectifier (by changing the load connected at the output terminals) in order to obtain an accurate representation of the exponential model. Therefore, the NLS optimization algorithm identifies the values by fitting the curves of three operating points of the rectifier. Figure 7 shows the corresponding Simulink model.

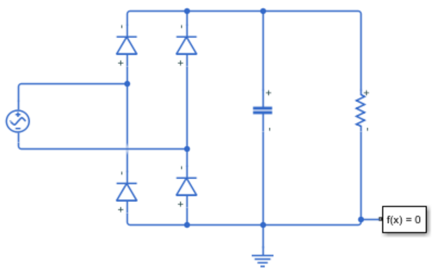

Figure 7. Simulink model of the single-phase rectifier

- Boost converter (open loop): The third stage of the proposed methodology is the estimation of the boost converter electrical components. The available data are the currents and voltages at the input terminals of the EMI filter and at the output of the boost converter. Therefore, the previously estimated parameters of the EMI filter and the rectifier are required in this optimization process. As explained in Subsection 2.1, the parasitic components must be considered in order to obtain accurate results.

 doi:10.20944/preprints202104.0617.v1

The data used in this stage is based on the steady state behavior of the converter when it is connected to a certain load. The timespan is chosen in order to increase the simulation speed without comprising the accuracy. Thus, the parameters can be estimated by analyzing a small number of periods (i.e. 2 or 3). The corresponding Simulink model is shown in Figure 8.

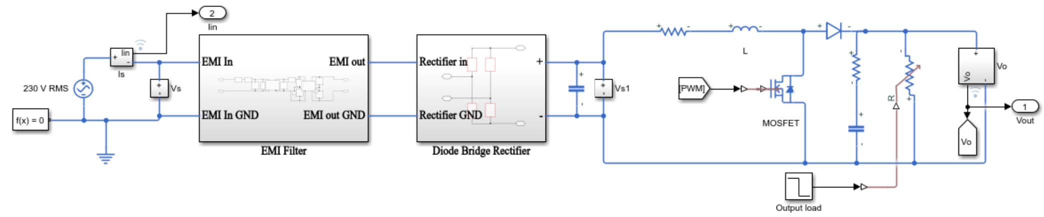

Figure 8. Simulink model of the boost PFC converter without control loop

- Control parameters (closed loop): The last stage consists of identifying the boost PFC control loop values that are listed in Subsection 2.1. It also re-estimates the value of the capacitor of the converter because it affects the transient response of the outer voltage loop [24]. It uses the estimated values of the previous stages and adds the voltage and current control loops to the Simulink model. The experimental setup is the same as in the open loop identification stage. However, the converter is subjected to a load change at the output terminal to obtain its transient response. The timespan of the data acquired is chosen depending on the time that the converter requires to reach the steady state. In this stage the NLS algorithm requires more time compared to the other stages, because it uses a model with a higher complexity and the dataset is larger. Figure 9 shows the corresponding Simulink model of the control loop that was added to the boost PFC presented in Figure 8.

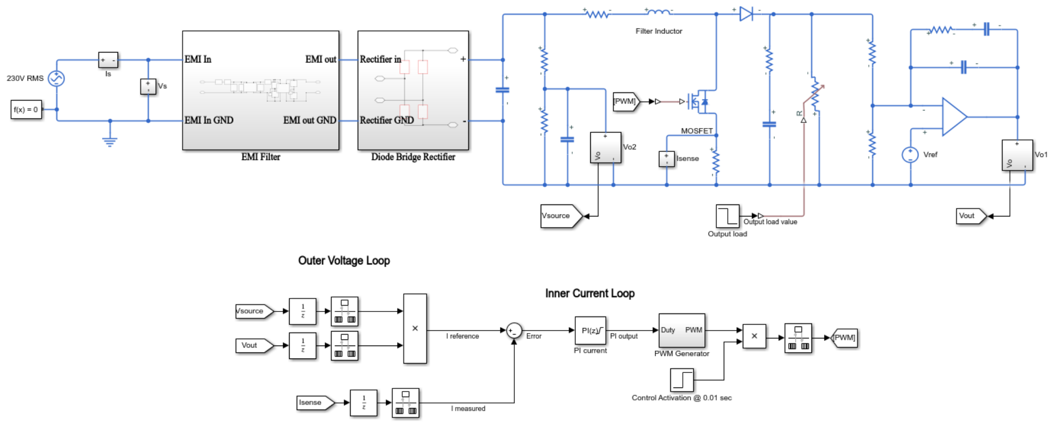

Figure 9. Simulink model of the boost PFC converter with the control loops

As shown in Figure 5, each stage of the proposed algorithm includes a data pre-processing step which is fundamental to run the optimization process. This step consists of resizing, filtering and synchronizing the raw data according to the data generated by the Simulink models. The resizing consists of reducing the number of points of the data measured without losing relevant information. It is done by means of an interpolation and it directly affects the computational burden of the process. After resizing the data, the next step is to eliminate the high-frequency noise by applying a low-pass finite impulse response filter as it is the moving average. The number of considered points depends on the type of data. Finally, the time vector of the measured signals is modified in order to synchronize the data generated from the simulations with the experimental data, which is essential for curve fitting purposes.

Another important aspect to consider is the definition of the seed point and the upper and lower boundaries of the variables to be identified. The selection of the initial point is based on a-priori knowledge of the different elements of boost PFC converters and the boundaries are set to cover six orders of magnitude, i.e. a typical initial value of the inductor in a boost converter is 1 μH, so that the lower and upper boundaries are set to 1 nH and 1 mH, respectively.

After each NLS optimization, the error value is compared to a fixed value δ that is selected at each stage of the proposed algorithm. This value is set to 0.01 for all stages. If the error value is higher than the defined threshold, the initial point and the constraints are modified by multiplying the obtained values by a random number between 0.75 and 1.25 and the NLS optimization starts again. This is done to assure that the process reaches a different local minimum than the last one. The algorithm advances to the next step when the error value is lower than δ, otherwise it iterates. Equation (5) defines the error, which is calculated based on the experimental and estimated values of the signals used in the optimization process.

$$error = \sum_{i=1}^{Sig} Mean\left(\left|\frac{x_{i,norm,\exp} - x_{i,norm,est}}{x_{i,norm,\exp}}\right|\right) \quad (5)$$

x refers the signals that are fitted in the NLS optimization. The values are normalized to have the voltages and currents of similar magnitudes, which allows a proper comparison.

4. Results

This section presents the experimental results obtained with the EMI filter and the boost PFC converter. For this purpose, the input and output voltages and currents were acquired under the conditions specified in the previous section.

As mentioned in Section 2, the EMI filter and boost PFC used in the laboratory for the parameter estimation process are the Corcom 10VN1 and the STMicroelectronics STEVAL-ISA102V2, respectively. The maximum rated voltage of the filter is 250 VAC, its rated current is in the range 6-10 A and the operating frequency could be 50 Hz or 60 Hz. The specifications of the boost PFC are listed in Table 1.

Table 1. STMicroelectronics STEVAL-ISA102V2 Boost PFC converter specifications.

Parameter	Value
Line voltage range	88 to 265 VAC
Output voltage	400 VDC
Rated output power	80 W
Switching frequency	35 kHz
Minimum efficiency	92%

The equipment used to measure the voltages and currents of the different devices consisted of a 4 channel oscilloscope (Tektronix MDO3024 200 MHz 2.5 GS/s; Tektronix, Beaverton, OR, USA), two high-frequency current probes (Tektronix TCP0030A 0.001-20 A 120 MHz; Tektronix, Beaverton, OR, USA) and two high-frequency differential probes (Tektronix THDP200; Tektronix, Beaverton, OR, USA).

Figure 10 presents the experimental setup used to acquire the necessary data for the parameter estimation process. Figure 10 (a) shows the setup used for the EMI filter identification stage of the proposed methodology, while the experimental setup presented in 10 (b) is used for the identification of the other stages of the methodology.

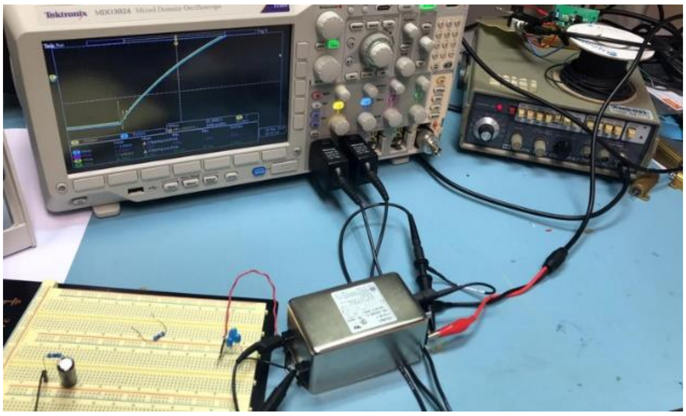

(a)

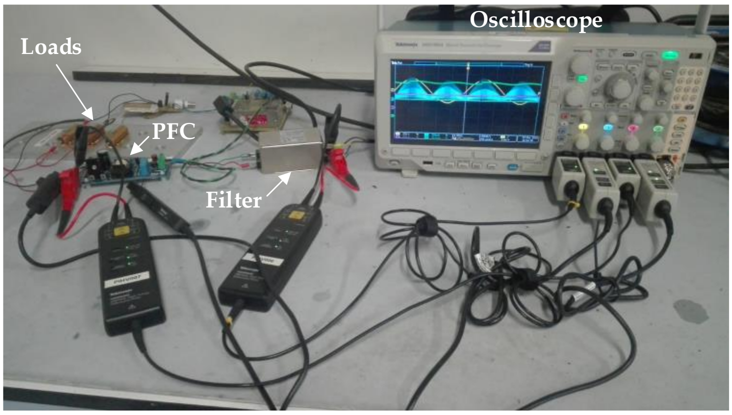

(b)

Figure 10. Experimental setup meant for the: **(a)** Corcom 10VN1 EMI filter parameter estimation; **(b)** STMicroelectronics STEVAL-ISA102V2 AC-DC boost PFC converter connected to the EMI filter

4.1. EMI filter parameter identification

According to the methodology presented in Figure 5, the parameter identification of the EMI filter is the first stage of the process. To this end, the data is acquired based on the procedure explained in Subsection 3.2. The periodic square wave voltage applied to the filter has an amplitude of 2 V and a frequency of 50 Hz, while the load consists of an 11 µF capacitor connected in parallel to an 11 Ω resistor. Table 2 presents the minimum, maximum, initial and optimal (identified) values of the NLS optimization algorithm. It also shows the theoretical values given by the manufacturer. The simulation time was of 8 hours and 42 minutes approximately, using an Intel® Xeon® CPU, ES.1650 v2 3.50 GHz, with 64 GB of RAM memory.

Table 2. Optimization conditions of the NLS identification algorithm of the EMI filter and comparison of actual and identified parameters.

Parameter	Minimum (*lb*)	Maximum (*ub*)	Initial	Actual (datasheet)	Identified	Error
R	1 Ω	1 MΩ	1 kΩ	270 kΩ	260.15 kΩ	3.67 %
C_1	1 nF	1 mF	1 µF	0.68 µF	0.62 µF	8.82 %
C_2	1 nF	1 mF	1 µF	0.47 µF	0.45 µF	4.26 %
C_3	1 nF	1 mF	1 µF	0.01 µF	0.0103 µF	3 %
C_4	1 nF	1 mF	1 µF	0.01 µF	0.0103 µF	3 %
C_5	1 nF	1 mF	1 µF	0.0055 µF	0.0047 µF	14.5 %
C_6	1 nF	1 mF	1 µF	0.0055 µF	0.0047 µF	14.5 %
L_1	10 nH	10 mH	10 µH	6.36 mH	6.42 mH	0.94 %
L_2	10 nH	10 mH	10 µH	6.36 mH	6.42 mH	0.94 %
L_3	10 nH	10 mH	10 µH	0.06 mH	0.059 mH	1.7 %
L_4	10 nH	10 mH	10 µH	1.47 mH	1.35 mH	8.16 %
L_5	10 nH	10 mH	10 µH	1.47 mH	1.35 mH	8.16 %

Figures 11 and 12 show the experimental and estimated signals at the input and output terminals of the EMI filter, as well as the Bode magnitude and phase plots of the filter. The estimation is done by simulating the electrical model of Figure 2 using the identified parameters presented in Table 2. The results show a good agreement between experimental and simulated results considering the identified parameters. It is also appreciated that the frequency response is almost the same for both cases.

Preprints (www.preprints.org) | NOT PEER-REVIEWED | Posted: 22 April 2021 doi:10.20944/preprints202104.0617.v1

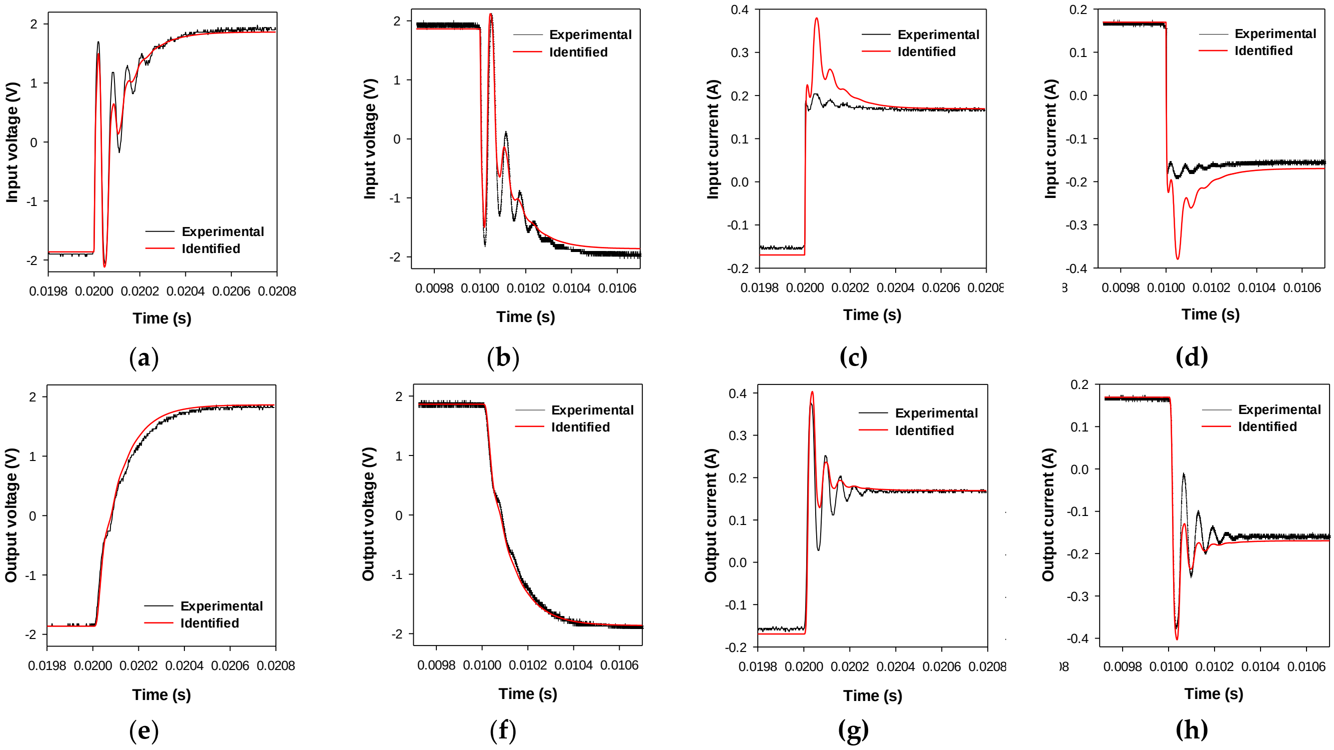

Figure 11. EMI filter. Experimental versus simulated data using the identified parameters. **(a)** Rising edge input voltage; **(b)** Falling edge input voltage; **(c)** Rising edge input current; **(d)** Falling edge input current; **(e)** Rising edge output voltage; **(f)** Falling edge output voltage; **(g)** Rising edge output current; **(h)** Falling edge output current.

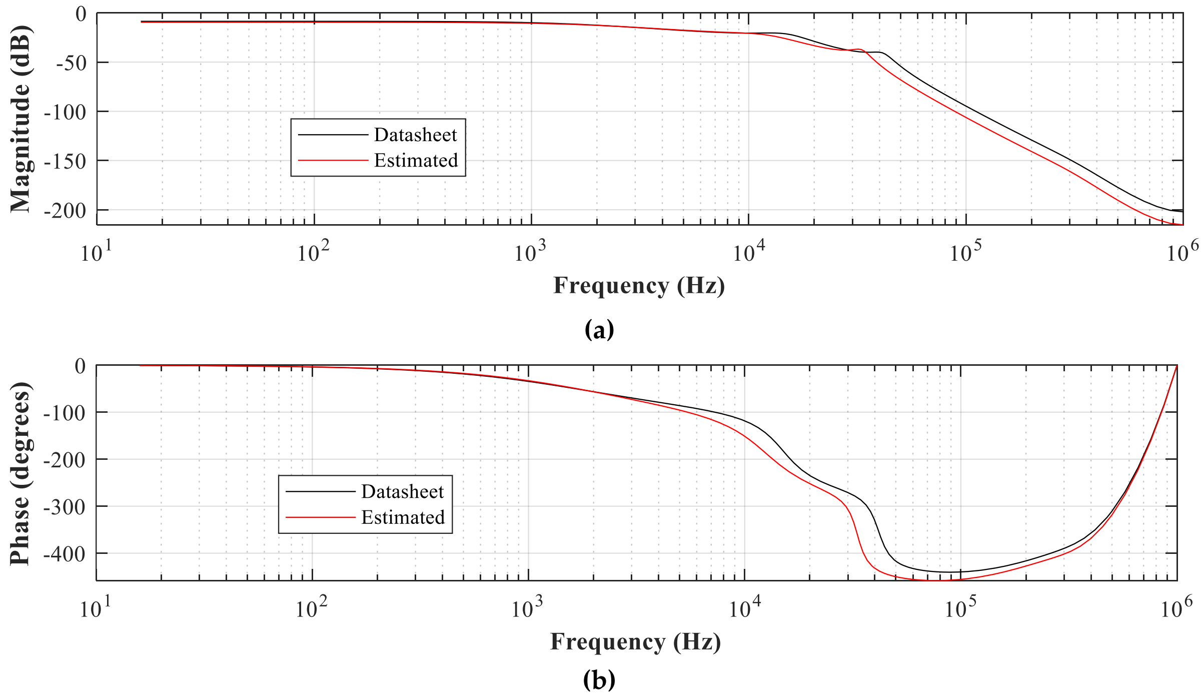

Figure 12. Comparison of the actual and the estimated bode plot of the EMI filter: **(a)** Magnitude; **(b)** Phase.

4.2. Rectifier parameter identification

Since the single phase rectifier is integrated in the evaluation module of the boost PFC used in this paper, the data acquired in this stage of the proposed methodology is based on the experimental setup presented in Figure 10 (b). However, the EMI filter is not used and the voltage and current probes are placed at the input of the boost PFC and at the smooth capacitor. The rectifier is fed with an input signal of 230 V and 50 Hz. As mentioned in Subsection 3.2, the rectifier must be tested under different operating points due to the requirements of the exponential model of the diode, thus, the output loads were selected to 3.9 kΩ, 1.95 kΩ and 7.8 kΩ. The simulation time was of about 1 hour and 7 minutes, which is relatively fast considering the type of problem.

Table 3 presents the main values of the NLS optimization procedure and compares the optimal point to the actual values of the rectifier. It is important to mention that some values are not provided by the manufacturer.

Table 3. Optimization conditions of the NLS identification algorithm of the single-phase rectifier and comparison of actual and identified parameters.

Parameter	Minimum (*lb*)	Maximum (*ub*)	Initial	Actual (datasheet)	Identified	Error
I_S	1 pA	1 mA	1 µA	-	4.86 mA	-
T_m	270 K	350 K	300 K	-	328.2 K	-
N	0	2	1	-	0.1494	-
R_{diode}	1 µΩ	1 Ω	1 mΩ	-	12 mΩ	-
C_{smooth}	1 nF	1 mF	1 µF	0.22 µH	0.2112 µH	4 %

There is not available data regarding the theoretical values of the rectifier parameters. Thus, it is necessary to compare the measured output voltage and current with estimated ones, as done in Figure 13. It is seen that the estimation reproduces with high fidelity the amplitude, mean value and frequency of the output signals of the single-phase rectifier. Figure 13 (c) shows that the high-frequency switching characteristics of the output current are also replicated with accuracy. Figure 14 shows the estimation of the forward I-V curve of the diode, which is calculated using the identified parameters, and it is compared with the forward I-V curve provided by the manufacturer.

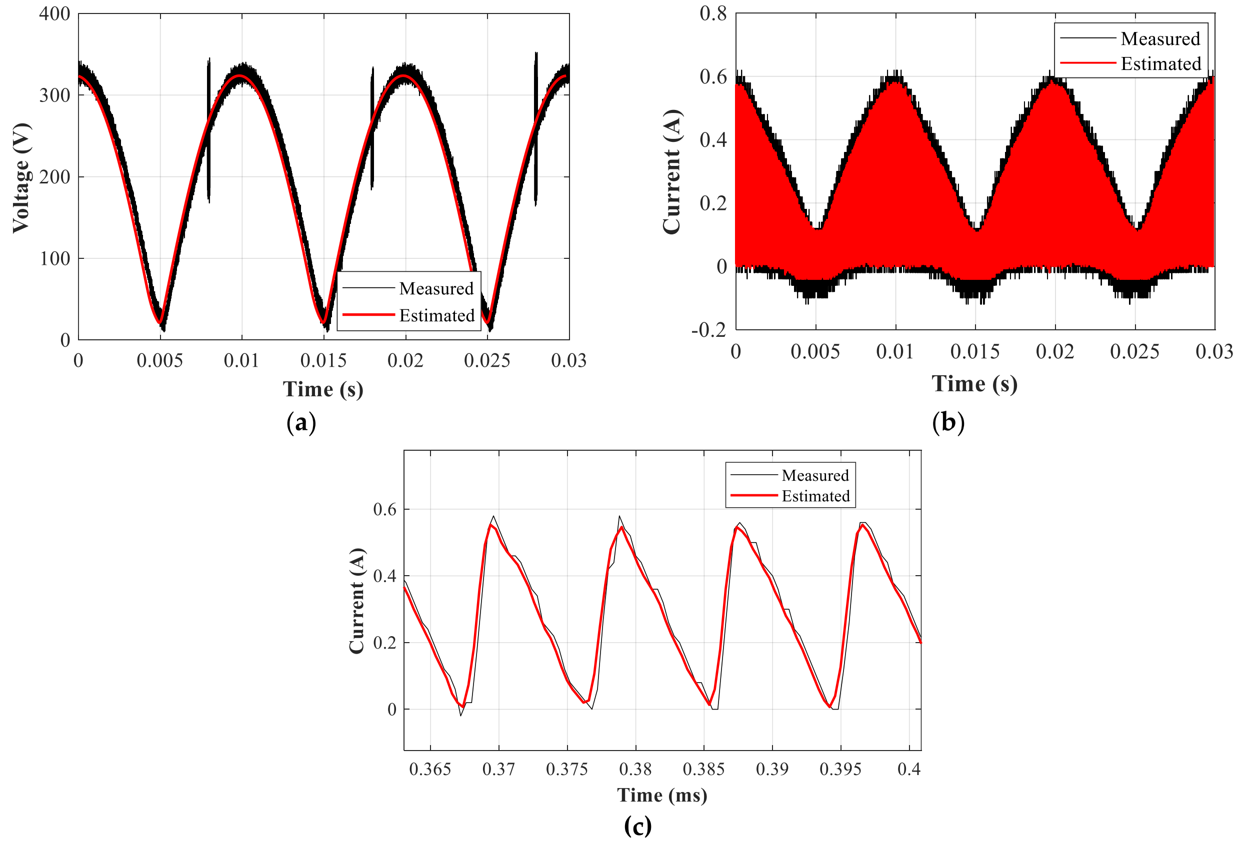

Figure 13. Measured and estimated waveforms of the rectifier. **(a)** Output voltage; **(b)** Output current; **(c)** Output current switching characteristics.

Preprints (www.preprints.org) | NOT PEER-REVIEWED | Posted: 22 April 2021 doi:10.20944/preprints202104.0617.v1

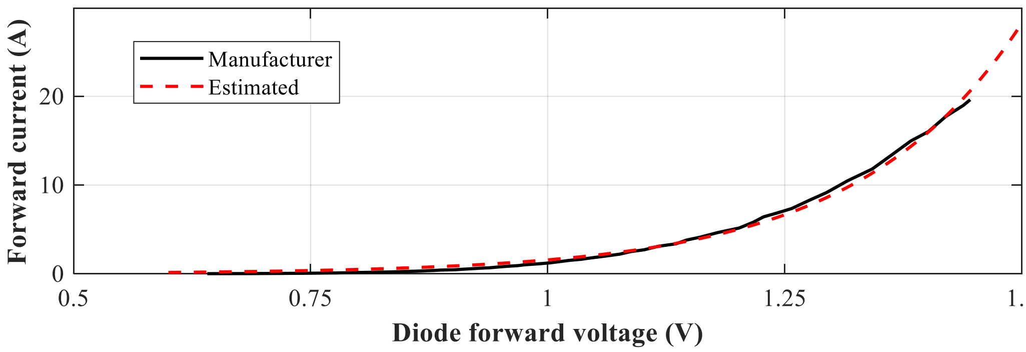

Figure 14. Manufacturer and estimated I-V curves of the rectifier diodes

4.3. Boost converter parameter identification

After identifying the parameters of the input filter and the AC-DC rectifier, the next stage of the proposed methodology is the identification of the steady state parameters of the boost PFC converter. The procedure explained in Subsection 3.2 is carried out and the data is measured using the setup presented in Figure 10 (b). A load of 3.9 kΩ was connected to the output of the converter and the timespan of the measurements is equivalent to three times the switching period of the boost converter. The duty cycle value is fixed to 0.12 given that the control loop is not considered in this stage.

Table 4 presents the values of the initial point and boundaries of the variables, as well as the comparison between the estimated and actual values of the passive elements. The simulation lasted for about 2 hours and 56 minutes.

Table 4. Optimization conditions of the NLS identification algorithm of the boost converter and comparison of actual and identified parameters.

Parameter	Minimum (lb)	Maximum (ub)	Initial	Actual (datasheet)	Identified	Error
C	1 nF	1 mF	1 µF	47 µF	33.2	29.4 %
R_C	1 µΩ	1 Ω	1 mΩ	19.4 mΩ	20.02 mΩ	3.20 %
L	10 nH	10 mH	10 µH	0.7 mH	0.701 mH	0.14 %
R_L	1 µΩ	1 Ω	1 mΩ	-	9.72 mΩ	-
R_{S1}	1 µΩ	1 Ω	1 mΩ	860 mΩ	882.8 mΩ	2.65 %
R_{S2}	1 µΩ	1 Ω	1 mΩ	-	114.2 mΩ	-

The results presented in Table 4 show a high accuracy in the identification of the parameters of the boost converter except for the capacitor. However, as it was mentioned above, this parameter also affects the transient behavior of the converter, thus, it is re-identified in the next stage of the process.

Figure 15 presents the measurement and steady-state estimation of the input and output signals of the converter. It is appreciated that the estimated curves fit the acquired data with high precision and the ripple of the signals is the same.

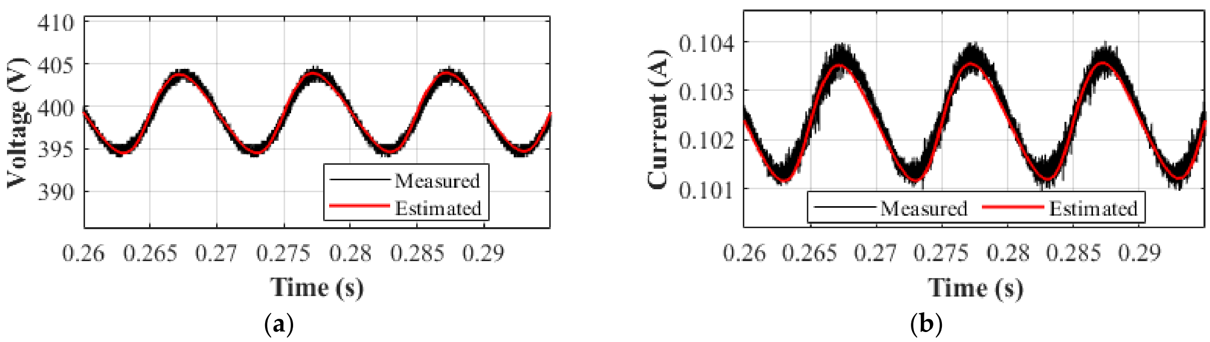

Preprints (www.preprints.org) | NOT PEER-REVIEWED | Posted: 22 April 2021 doi:10.20944/preprints202104.0617.v1

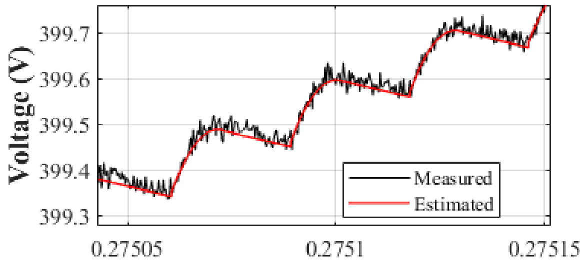

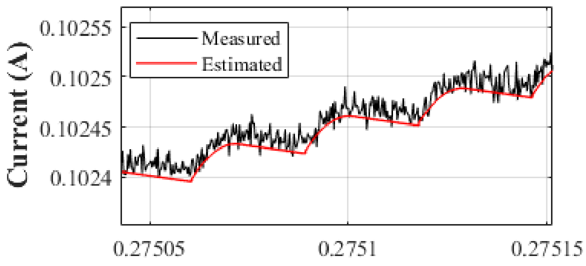

Figure 15. Experimental versus simulated data of the boost converter: (a) Output voltage (timespan is three periods of AC source frequency); (b) Output current (timespan is three periods of AC source frequency); (c) Output voltage (timespan is three periods of the PWM switching frequency); (d) Output current (timespan is three periods of the PWM switching frequency).

4.4. Control loop parameter identification

The last stage of the identification procedure consists of finding the parameters related to the outer voltage and inner current control loop. It uses the models and identified values from the EMI filter, the rectifier and the boost converter in order to estimate the controller parameters. The experimental setup presented in Figure 10 (b) is used to acquire the data. A sudden load change is applied to capture the transient response of the boost PFC. The output load of the converter changes from 3.9 kΩ to 1.95 kΩ and the timespan of the measurements is defined according to the time that the converter needs to reach the steady state. As mentioned in the previous subsection, the value of the boost converter capacitor is also identified in this stage, and its initial value is the estimated value obtained in the previous stage.

Table 5 shows the initial, minimum, maximum, estimated and theoretical values of the controller parameters. The actual proportional and integral constants are not specified because they are not given by the manufacturer. The time required in this optimization was 7 hours and 46 minutes.

Table 5. Optimization conditions of the NLS identification algorithm of the control loop and comparison of actual and identified parameters.

Parameter	Minimum (lb)	Maximum (ub)	Initial	Actual (datasheet)	Identified	Error
C	1 µF	100 µF	33.2 µF	47 µF	44.2 µF	5.96 %
R_1	10 Ω	10 MΩ	10 kΩ	2 MΩ	1.973 MΩ	1.35 %
R_2	10 Ω	10 MΩ	10 kΩ	15 kΩ	14.82 kΩ	1.2 %
R_3	10 Ω	10 MΩ	10 kΩ	2 MΩ	2.05 MΩ	2.5 %
R_4	10 Ω	10 MΩ	10 kΩ	12.7 kΩ	12.002 kΩ	5.50 %
R_5	10 Ω	10 MΩ	10 kΩ	22 kΩ	22.36 kΩ	1.64 %
C_1	1 nF	1 mF	1 µF	10 nF	9.38 nF	6.2 %
C_2	1 nF	1 mF	1 µF	2200 nF	2096.5 nF	4.7 %
C_3	1 nF	1 mF	1 µF	150 nF	148.3 nF	1.13 %
K_P	10^{-6}	10^{6}	1	-	0.0892	-
K_I	10^{-6}	10^{6}	1	-	1258.5	-

The results in Table 5 show that the identified value of the boost PFC capacitor is more accurate than the estimation in the previous stage, while the values of the outer voltage control loop are identified with high precision.

Figure 16 compares the measured and estimated curves when a load change occurs. It is appreciated that the signals simulated with the identified parameters are able to replicate the behavior of the boost PFC converter.

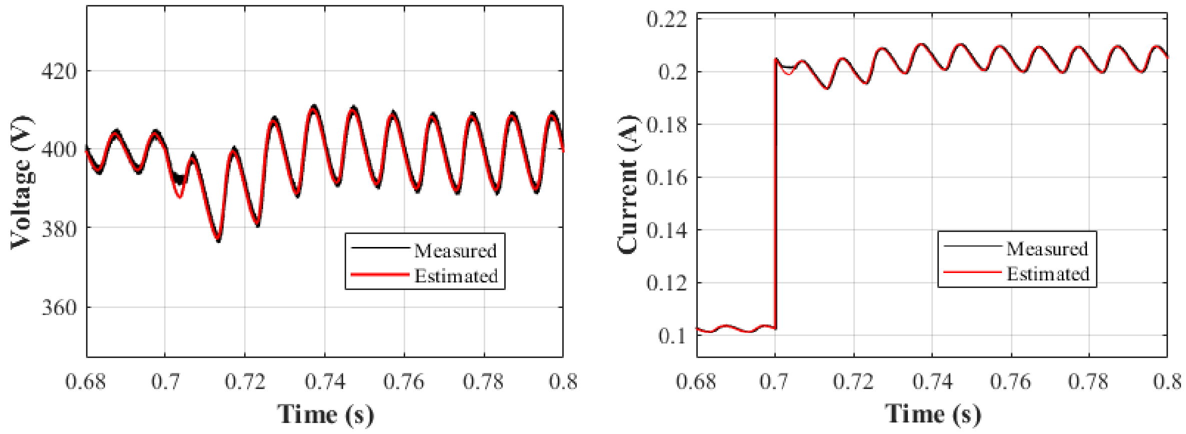

(**a**) (**b**)

Figure 16. Measured and simulated transient response of the boost PFC. (a) Input voltage. (b) Input current.

The average relative error of the estimated parameters is 4.473 %, which has been calculated based on the error values presented in Tables 2 to 5. Finally, the error of the fitting process is 0.00082, which has been calculated by applying Equation (5) to the signals displayed in Fig. 16 (a) and (b). Note that this value is more than ten times below the defined threshold $\delta = 0.01$.

5. Conclusions

Accurate modeling of power factor corrector converters is very important in sectors where power consumption due to electronic power loads is significant. This may lead to improved designs, implementation of better control strategies or fulfillment of industry standards, among many other advantages. This paper has presented a parameter identification strategy of a boost PFC converter integrating an EMI filter at the input stage. This approach uses the trust-region nonlinear least squares optimization algorithm, the topology of the circuits and non-intrusive measurements at the input and output terminals of the device. More than 30 parameters were identified with high precision and the behavior of the AC-DC converter was replicated with high accuracy. The experimental results show that the average relative error of the identified parameters was below 5 %, which proves the accuracy of the proposed approach. This methodology can be applied to other power electronics devices.

Author Contributions: Conceptualization, M.M.-E. and G.R.-D..; methodology, J.-R.R.; formal analysis, M.M.-E. and J.-R.R..; investigation, J.-R.R. and G.R.-D..; writing—original draft preparation, G.R.-D. and J.-R.R.; writing—review and editing, M.M.-E and G.T.-D. All authors have read and agreed to the published version of the manuscript.

Funding: This research was funded by Generalitat de Catalunya, grant number SGR 2017 SGR 967 and the European Commission through the Clean Sky program, grant number 755332-AEMS-IdFit.

Conflicts of Interest: The authors declare no conflict of interest.

References

1. Bodetto, M.; Aroudi, A.E.; Cid-Pastor, A.; Calvente, J.; Martínez-Salamero, L. Design of AC-DC PFC high-order converters with regulated output current for low-power applications. *IEEE Trans. Power Electron.* **2016**, *31*, 2012–2025, doi:10.1109/TPEL.2015.2434937.
2. Ren, X.; Wu, Y.; Guo, Z.; Zhang, Z.; Chen, Q. An Online Monitoring Method of Circuit Parameters for Variable On-Time Control in CRM Boost PFC Converters. *IEEE Trans. Power Electron.* **2019**, *34*, 1786–1797, doi:10.1109/TPEL.2018.2828988.
3. Bayona, J.; Gélvez, N.; Espitia, H. Design, Analysis, and Implementation of an Equalizer Circuit for the Elimination of Voltage Imbalance in a Half-Bridge Boost Converter with Power Factor Correction. *Electronics* **2020**, *9*, 2171,

doi:10.3390/electronics9122171.
4. Bao, J.; Liu, J.; Huang, Z.; Liu, W.; Li, H. An Online Parameter Identification for Ultracapacitor Model by Using Recursive Least Square with Multi-forgetting Factor. In Proceedings of the 2018 13th World Congress on Intelligent Control and Automation (WCICA); IEEE, 2018; pp. 962–966.
5. Xu, H.; Chen, D.; Xue, F.; Li, X. Optimal design method of interleaved boost PFC for improving efficiency from switching frequency, boost inductor, and output voltage. *IEEE Trans. Power Electron.* **2019**, *34*, 6088–6107, doi:10.1109/TPEL.2018.2872427.
6. Kotny, J.-L.; Margueron, X.; Idir, N. High-Frequency Model of the Coupled Inductors Used in EMI Filters. *IEEE Trans. Power Electron.* **2012**, *27*, 2805–2812, doi:10.1109/TPEL.2011.2175452.
7. Riba, J.; Moreno-eguilaz, M.; Bogarra, S.; Garcia, A. Parameter Identification of DC-DC Converters under Steady-State and Transient Conditions Based on White-Box Models. *Electronics* **2018**, *7*, doi:10.3390/electronics7120393.
8. Valdivia, V. Behavioral Modeling and Identification of Power Electronics Converters and Subsystems Based on Transient Response, Carlos III (Madrid), 2013.
9. Oliver, J.A.; Prieto, R.; Romero, V.; Cobos, J.A. Behavioural Modelling of DC-DC Converters for Large-Signal Simulation of Distributed Power Systems. *Twenty-First Annu. IEEE Appl. Power Electron. Conf. Expo. 2006. APEC '06.* **2006**, 1204–1209, doi:10.1109/APEC.2006.1620692.
10. Wang, L.; Deng, X.; Han, P.; Qi, X.; Wu, X.; Li, M.; Xu, H. Electromagnetic Transient Modeling and Simulation of Power Converters Based on a Piecewise Generalized State Space Averaging Method. *IEEE Access* **2019**, *7*, 12241–12251, doi:10.1109/ACCESS.2019.2891122.
11. Nabinejad, A.; Rajaei, A.; Mardaneh, M. A Systematic Approach to Extract State-Space Averaged Equations and Small-Signal Model of Partial-Power Converters. *IEEE J. Emerg. Sel. Top. Power Electron.* **2020**, *8*, 2475–2483, doi:10.1109/JESTPE.2019.2915248.
12. Ahmeid, M.; Armstrong, M.; Gadoue, S.; Algreer, M.; Missailidis, P.; Al-Greer, M.; Missailidis, P. Real-Time Parameter Estimation of DC–DC Converters Using a Self-Tuned Kalman Filter. *IEEE Trans. Power Electron.* **2017**, *32*, 5666–5674, doi:10.1109/TPEL.2016.2606417.
13. Algreer, M.; Armstrong, M.; Giaouris, D. Active Online System Identification of Switch Mode DC–DC Power Converter Based on Efficient Recursive DCD-IIR Adaptive Filter. *IEEE Trans. Power Electron.* **2012**, *27*, 4425–4435, doi:10.1109/TPEL.2012.2190754.
14. Buiatti, G.M.; Amaral, A.M.R.; Cardoso, A.J.M. An unified method for estimating the parameters of non-isolated DC/DC converters using continuous time models. *Telecommun. Energy Conf. 2007. INTELEC 2007. 29th Int.* **2007**, 334–341, doi:10.1109/INTLEC.2007.4448794.
15. Rojas-Duenas, G.; Riba, J.-R.; Kahalerras, K.; Moreno-Eguilaz, M.; Kadechkar, A.; Gomez-Pau, A. Black-Box Modelling of a DC-DC Buck Converter Based on a Recurrent Neural Network. In Proceedings of the 2020 IEEE International Conference on Industrial Technology (ICIT); Institute of Electrical and Electronics Engineers (IEEE): Buenos Aires, 2020; pp. 456–461.
16. Rojas-Dueñas, G.; Riba, J.-R.; Moreno-Eguilaz, M. Non-Linear Least Squares Optimization for Parametric Identification of DC-DC Converters. *IEEE Trans. Power Electron.* **2021**, *36*, 654–661, doi:10.1109/tpel.2020.3003075.
17. Al-Greer, M.; Armstrong, M.; Ahmeid, M.; Giaouris, D. Advances on system identification techniques for DC-DC switch mode power converter applications. *IEEE Trans. Power Electron.* **2019**, *34*, 6973–6990, doi:10.1109/TPEL.2018.2874997.
18. Labarre, C.; Costa, F. Circuit analysis of an EMI filter for the prediction of its magnetic near-field emissions. *IEEE Trans. Electromagn. Compat.* **2012**, *54*, 290–298, doi:10.1109/TEMC.2011.2159563.
19. Wang, N.; Yan, Z.; Tang, J.; Ning, Z.; Xiao, B.; Wang, H. Study on Prediction Models of EMI Filter with Near-field Coupling Effect. In Proceedings of the 2018 12th International Symposium on Antennas, Propagation and EM Theory, ISAPE 2018 - Proceedings; Institute of Electrical and Electronics Engineers Inc., 2019.

20. Narayanasamy, B.; Luo, F.; Chu, Y. Modeling and Stability Analysis of Voltage Sensing based Differential Mode Active EMI Filters for AC-DC Power Converters. In Proceedings of the 2018 IEEE Symposium on Electromagnetic Compatibility, Signal Integrity and Power Integrity, EMC, SI and PI 2018; Institute of Electrical and Electronics Engineers Inc., 2018.
21. Zhang, R.; Ma, W.; Wang, L.; Hu, M.; Cao, L.; Zhou, H.; Zhang, Y. Line Frequency Instability of One-Cycle-Controlled Boost Power Factor Correction Converter. *Electronics* **2018**, *7*, 203, doi:10.3390/electronics7090203.
22. Singh, A.; Mallik, A.; Khaligh, A. A Comprehensive Design and Optimization of the DM EMI Filter in a Boost PFC Converter. In Proceedings of the IEEE Transactions on Industry Applications; Institute of Electrical and Electronics Engineers Inc., 2018; Vol. 54, pp. 2023–2031.
23. Pelz, B.; Belkadi, A.; Moddel, G. Avoiding erroneous analysis of MIM diode current-voltage characteristics through exponential fitting. *Meas. J. Int. Meas. Confed.* **2018**, *120*, 28–33, doi:10.1016/j.measurement.2018.01.054.
24. Chu, G.; Tse, C.K.; Wong, S.C.; Tan, S.C. A unified approach for the derivation of robust control for boost PFC converters. *IEEE Trans. Power Electron.* **2009**, *24*, 2531–2544, doi:10.1109/TPEL.2009.2020986.
25. Lee, S.W.; Management, P. *Application Report Demystifying Type II and Type III Compensators Using Op-Amp and OTA for DC/DC Converters*; 2014;
26. Alonge, F.; D'Ippolito, F.; Raimondi, F.M.; Tumminaro, S. Nonlinear modeling of DC/DC converters using the Hammerstein's approach. *IEEE Trans. Power Electron.* **2007**, *22*, 1210–1221, doi:10.1109/TPEL.2007.900551.
27. Le, T.M.; Fatahi, B.; Khabbaz, H.; Sun, W. Numerical optimization applying trust-region reflective least squares algorithm with constraints to optimize the non-linear creep parameters of soft soil. *Appl. Math. Model.* **2017**, *41*, 236–256, doi:10.1016/j.apm.2016.08.034.
28. Wu, L.; Chen, Z.; Long, C.; Cheng, S.; Lin, P.; Chen, Y.; Chen, H. Parameter extraction of photovoltaic models from measured I-V characteristics curves using a hybrid trust-region reflective algorithm. *Appl. Energy* **2018**, *232*, 36–53, doi:10.1016/j.apenergy.2018.09.161.
29. Ahsan, M.; Choudhry, M.A. System identification of an airship using trust region reflective least squares algorithm. *Int. J. Control. Autom. Syst.* **2017**, *15*, 1384–1393, doi:10.1007/s12555-015-0409-0.